A R C H I V E O F M E C H A N I C A L E N G I N E E R I N G

Volume 68 2021 Number 1

DOI: 10.24425/ame.2020.131707

Key words: grey relational analysis, principal component analysis, Taguchi method, analysis of variance, cryogenic cooling

Mst. Nazma Sultana[1], Nikhil Ranjan Dhar[1]

Hybrid GRA-PCA and modified weighted TOPSIS coupled with Taguchi for multi-response process parameter optimization in turning AISI 1040 steel

The objective of the present study is to optimize multiple process parameters in turning for achieving minimum chip-tool interface temperature, surface roughness and specific cutting energy by using numerical models. The proposed optimization models are offline conventional methods, namely hybrid Taguchi-GRA-PCA and Taguchi integrated modified weighted TOPSIS. For evaluating the effects of input process parameters both models use ANOVA as a supplementary tool. Moreover, simple linear regression analysis has been performed for establishing mathematical relationship between input factors and responses. A total of eighteen experiments have been conducted in dry and cryogenic cooling conditions based on Taguchi L18 orthogonal array. The optimization results achieved by hybrid Taguchi-GRA-PCA and modified weighted TOPSIS manifest that turning at a cutting speed of 144 m/min and a feed rate of 0.16 mm/rev in cryogenic cooling condition optimizes the multi-responses concurrently. The prediction accuracy of the modified weighted TOPSIS method is found better than hybrid Taguchi-GRA-PCA using regression analysis.

1. Introduction

AISI 1040 steel is popularly utilized for producing crank shafts, automobile axles, spindles, and lightly stressed gears etc. But, at higher speed and feed rate, excessive heat generation under dry machining hampers machinability [1]. Application of cutting fluids is one of the possible solutions, but conventional cooling involves higher cost with environmental pollution as well as damage to human health [2]. Cryogenic cooling with liquid nitrogen (LN_2) is now practiced as a popular cooling technique in turning [3], milling [4], drilling [5], and grinding [6]

✉ Mst. Nazma Sultana, e-mails: nazma.kuet@yahoo.com; n.sultana@iem.kuet.ac.bd

[1]Bangladesh University of Engineering & Technology, Dhaka, Bangladesh.

due to its some attractive features. Despite of having some complexity of handling (without genuine pressure relief valve explosion may occur) the proper temperature and pressure with minor health hazards (due to extremely low temperature skin problems may arise) liquid nitrogen (LN_2) is almost absorbed by nature (because natural air comprises 78% N_2) with no direct bad effect on environment [7]. Moreover, owing to less disposal hassles, cryogenic cooling is selected as the cooling technique in this research. Turning is the oldest machining process and plays a notable role in manufacturing [8]. The turning performances can be expressed in terms of chip-tool interface temperature, roughness, tool wear, specific cutting energy, coefficient of friction, cutting force, chip thickness, MRR etc., and those performances are affected by the process parameters such as speed, feed rate, depth of cut, cutting environment, tool and work material. In a word, for achieving desired machinability, appropriate selection of process parameters is mandatory.

Taguchi method (TM) is one of the most widespread and constructive optimization tools due to its low time-consuming design of experiments (DoE) and less complexity of computation [9]. But the significance rate of input factors on responses cannot be determined by TM, while it can be solved by adding analysis of variance (ANOVA) as a supplementary tool. Besides, another drawback of TM is that this method cannot deal with multi-responses at a time. To pursue this objective, various multi-response optimization tools such as Taguchi-DEAR (Data Envelopment Analysis based Ranking), response surface methodology (RSM), artificial neural network (ANN), grey relational analysis (GRA), technique for order of preference by similarity to ideal solutions (TOPSIS), particle swarm optimization (PSO) can be applied. Taguchi-DEAR is one of the simplest optimization tool, but it can only deal with conflicting characteristics of responses [10]. RSM is an effective optimization method, but its lengthy computation is very troublesome [11]. The prediction accuracy of ANN is higher with a larger number of trials, but this is time-consuming [12]. GRA is able to optimize process with less information, but the same weights are considered for all responses, which is not practical [13]. TOPSIS can optimize multiple responses, but in it assigning weights to responses is vague [14]. PSO is a straightforward simple method, but its tendency to wander during optimization limits its applications [15].

Recently, among these optimization methods, GRA and TOPSIS are coupled with TM by researchers in different process optimization at a growing rate. Meral et al. [16] optimized process parameters in drilling of AISI 4140 steel using Taguchi method for mono-objective optimization and Taguchi based GRA for multi-objective optimization. Priyadarshini et al. [17] studied energy consumption, MRR and surface roughness in turning mild steel with high-speed steel tool material and optimized those responses using Taguchi-supported fuzzy TOPSIS. In this research work, two different weight assigning methods (principal component analysis (PCA) and modified standard deviation method) are selected for diminishing the drawbacks of Taguchi-GRA and Taguchi-TOPSIS, respectively. PCA assists

Taguchi-GRA by computing relative weights of each assigned response [10]. Conversely modified standard deviation method is selected to obtain a better accuracy than in entropy weight method, so to expand the application of TOPSIS [18]. Details of recent research related to process parameter optimization in turning using Taguchi-GRA-PCA and TOPSIS are shortlisted in Table 1.

Table 1.
Lists of some reviewed papers on optimization of turning AISI 1040 using Taguchi-GRA-PCA and TOPSIS

References	Work material cooling method	Optimization tool	Input factors	Outputs
[19]	AISI 1060 steel, HPC	Taguchi-GRA-PCA	Speed, feed and depth of cut	Temperature, force, roughness, material removal rate (MRR)
[20]	Ti-6Al-4V, dry	Taguchi-GRA-Kernel PCA	Inserts type, feed and depth of cut	Thrust force, power, friction coefficient
[21]	AISI 52100, dry	Taguchi-GRA-PCA	Speed, feed, depth of cut, nose radius	Temperature, force, roughness
[22]	AISI 4340 steel, MQL	Taguchi-GRA-PCA	Speed, feed, depth of cut, nose radius	Force, roughness
[23]	Mg AZ 31D alloy, dry	Taguchi-GRA-PCA	Speed, feed and depth of cut	Force, roughness, MRR, tool wear
[24]	Mg AZ 31D alloy, dry	TOPSIS with RSA	Speed, feed	Roughness, flank tool wear
[25]	Incoloy 800H	TOPSIS	Speed, feed and depth of cut	Roughness, micro-hardness, MRR
[26]	Inconel 718	Taguchi-TOPSIS	Speed, feed and depth of cut	Roughness, MRR

The abovementioned literature review reveals that little attention have been paid to optimization of performances (chip-tool interface temperature (θ), surface roughness (R_a) and specific cutting energy (E_{sp})) in turning AISI 1040 steel considering cutting condition (dry and cryogenic cooling) as an input factor using hybrid Taguchi-GRA-PCA. The optimization of turning process by Taguchi integrated modified weighted (based on standard deviation) TOPSIS is fully missing. After finding out those research shortages, the motivation of our research is as follows:

- To experimentally investigate the efficiency of cryogenic cooling over dry turning and to optimize the assigned responses by hybrid Taguchi-GRA-PCA and Taguchi integrated modified weighted TOPSIS.
- To determine the influence of process parameters using ANOVA and to compare the prediction accuracy of both optimization methods by a confirmation test.

2. Experimental details

2.1. Materials and methods

A rigid powerful HMT lathe (11 kW: NH22 HMT, India: maximum spindle speed 3000 rpm) has been used for turning a work-piece of AISI 1040 steel having a length of 750 mm and an initial diameter of 200 mm by uncoated carbide insert SNMG 120408-26TTS (tool signature: −6°, −6°, 6°, 6°, 15°, 75° and 0.8 mm) with PSBNR 2525 M12 tool holder at different speed-feed combinations recommended by tool manufacturers based on common industrial applications. In view of lower cost with high availability and less time consumption, only uncoated tungsten carbide inserts were considered for the analysis. The composition, hardness, ultimate tensile strength of work material has been determined by XR-F (X-ray fluorescence), universal testing machine (UTM) and hardness tester, respectively and is given in Table 2. The setup of LN_2-assisted cryogenic turning is based on the principle followed by [2] which is schematically shown in Fig. 1. LN_2 was stored in the XL-45 Dewar at fixed pressure of 10 bars and its storage capacity was 180L. The flow rate was 0.35 l/min while a relief valve was used for 1.5 bar

Table 2.

Chemical compositions, hardness and UTS of AISI 1040 steel

Material	% composition				Hardness (BHN)	Ultimate tensile strength, UTS (MPa)
	C	Mn	P	S	180	617.8
AISI 1040	0.41	0.70	0.04	0.05		

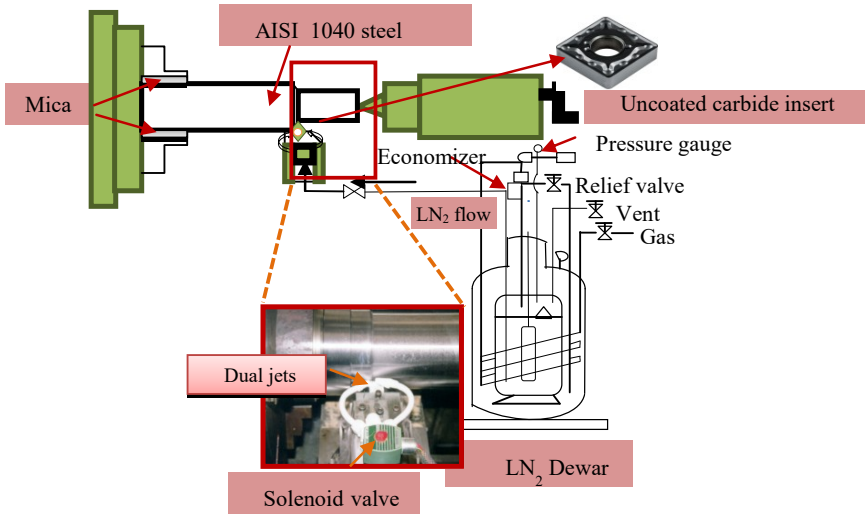

Fig. 1. Turning with liquid nitrogen-assisted dual jets cooling [2]

pressurized coolant supply. Highly insulated stainless steel hose carried out LN_2 from the Dewar to a nozzle, and a solenoid valve was attached just prior to the nozzle to control the flow on/off. 2.0 mm bore diameter sized nozzle with dual jets (0.5 mm each) supply was designed for cooling both the rake and flank faces of the cutting inserts.

2.2. Variables and responses

Chip-tool interface temperature (θ), arithmetic surface roughness (R_a) and specific cutting energy (E_{sp}) were considered as the responses. The reasons behind choosing those responses were: θ is the indication of heating status of cutting area which is the main malefactor of machinability, R_a is the quality representative index and E_{sp} is another influential factor of sustainability that indicates the requirement of energy for material cutting. The input process variables were the cutting speed, the feed rate and the cutting condition shown in Table 3. Due to the requirement of saving work material, the depth of cut was considered less significant and was kept fixed at 1.5 mm.

Table 3.

Input variables with their levels in turning

Notations	Variables	Units	No. of levels	Level 1	Level 2	Level 3
V_c	Cutting speed	m/min	3	85	110	144
S_0	Feed rate	mm/rev	3	0.16	0.20	0.24
CC	Cutting condition	–	2	Dry	Cryogenic	–

θ was measured by following the tool work thermocouple method through proper calibration during continuous chip formation. For proper calibration, a piece of long continuous chip and a tungsten carbide rod were brazed together as the thermocouple point instead of work material and carbide inserts. Heat sink was prepared by placing a graphite block on electrically-heated porcelain. Then, the brazed end and a reference K type thermocouple were attached on the top of graphite block. After heating, the heat sink the temperature of graphite block was measured directly by means of a digital temperature reading meter (Eurotherm, UK) connected to a reference thermocouple. The open end of the brazed chip and the tungsten carbide rod was linked with a digital multi-meter (Rishmulti 15s, India) which recorded the voltage. Afterwards, the graph of temperature against voltage was plotted in Fig. 2a for AISI 1040 steel and cutting insert. Finally, keeping in mind the above relations (the correlation between temperature and Emf is 99.9%), the chip tool interface temperature was measured, as shown in Fig. 2b. Surface roughness was checked out at three different positions on the turned surfaces in each experimental condition using a contact type roughness checker (Talysurf model: Surtronic 3P Rank Taylor Hobson Limited, UK) for achieving a better precision. Specific cutting energy (E_{sp}) was computed from the ratio of the principal cutting

force (F_c) to the product of feed rate (S_0) and the depth of cut (t), as shown in the equation below, and the cutting force was measured by 3-D dynamometer (KISTLER, 9257B type and charge amplifier: 5007) with a PC for data acquisition.

$$E_{sp} = \frac{F_c}{S_0 \times t} \left(\frac{\text{N}}{\text{mm}^2}\right). \tag{1}$$

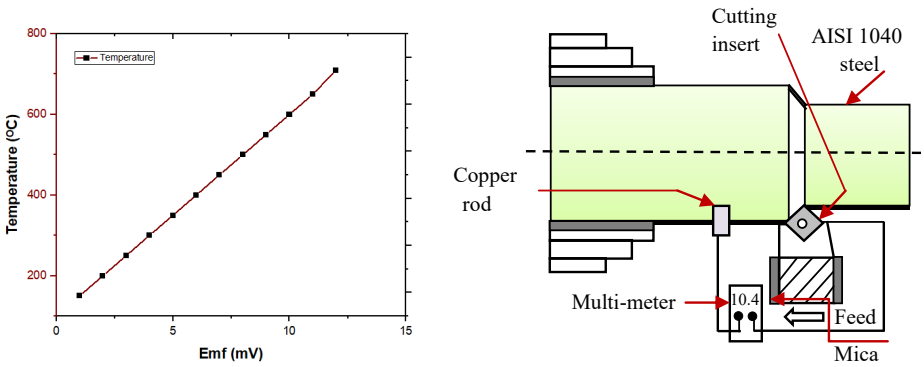

(a) (b)

Fig. 2. Calibration curve (a) and tool-work thermocouple setup (b)

3. Objectives and stepwise details of optimization models

3.1. Problem statements with objectives

Lower energy consumption is desirable during metal cutting. Within a certain range of increasing feed rate and depth of cut, a minimum E_{sp} can be achieved, but it increases R_a and θ [27]. For performing a trade-off among this three responses (θ, R_a, E_{sp}) it is hardly tried to optimize responses at a time within selected boundary conditions using hybrid Taguchi-GRA-PCA and Taguchi integrated modified weighted TOPSIS. Finally, the objectives with their boundary conditions are given below:

Objective function:

$$\text{minimize, } \theta, \ R_a, \ E_{sp}$$

boundary conditions,

$$85 \leq V_c \leq 144;$$
$$0.16 \leq S_0 \leq 0.24;$$
$$\text{CC} = \text{dry, cryogenic.}$$

Note that symbols are explained in Table 3.

3.2. Optimization models in detail

Detailed steps of optimization models are discussed briefly in the following subsections.

3.2.1. Hybrid Taguchi-GRA-PCA

Taguchi method is one of the popular statistical tools, developed by Dr. Genichi Taguchi [28], for parameter design with reducing the variation of quality characteristics to achieve the target result. In this research work, for evaluating multiple input factors, a Taguchi-based design of experiment (DoE) has been adopted, which contains L18 orthogonal array design structure for performing experimental trials, whose details have been listed in Table 4. In this method, the signal-to-noise (S/N) ratio has been mathematically used for optimizing the quality characteristics. Based on the current analysis the following principle is used for calculating the (S/N) ratio.

Table 4.

L18 orthogonal array of input variables (using SNMG 120408-26 TTS)

Experimental runs	V_c, m/min	S_0, mm/rev	CC	Experimental runs	V_c, m/min	S_0, mm/rev	CC
1.	85	0.16	Dry	10.	85	0.16	Cryogenic
2.	85	0.20	Dry	11.	85	0.20	Cryogenic
3.	85	0.24	Dry	12.	85	0.24	Cryogenic
4.	110	0.16	Dry	13.	110	0.16	Cryogenic
5.	110	0.20	Dry	14.	110	0.20	Cryogenic
6.	110	0.24	Dry	15.	110	0.24	Cryogenic
7.	144	0.16	Dry	16.	144	0.16	Cryogenic
8.	144	0.20	Dry	17.	144	0.20	Cryogenic
9.	144	0.24	Dry	18.	144	0.24	Cryogenic

Principle I: ‘Smaller the better’

$$\frac{S}{N} = -10 \log \frac{1}{n} \sum z^2, \tag{2}$$

where z is the representative of responses (θ, R_a, E_{sp}) and n is the total number of repetitive observations at each experimental run.

The next step is to synchronize GRA with Taguchi analysis. Grey relational analysis (GRA) was developed by Ju Long in 1982 utilizing the normalized (S/N) values obtained from Taguchi loss function for calculating grey relational coefficients (GRCs) and finally for defining ranks based on grey relational grade (GRG).

Three most popular computation stages of grey relational analysis (GRA) are described below:

Stage I (Data pre-processing): Converting responses into dimensionless form ranging from 0 to 1 based on the situation: 'smaller the better' and 'larger the better' [29]. In this study, all responses are normalized with 'smaller the better' objective using the following equation [29].

$$y_i(k) = \frac{\max S_i(k) - S_i(k)}{\max S_i(k) - \min S_i(k)}, \tag{3}$$

where $S_i(k)$ represents the (S/N) value of individual responses in each experimental run $i = 1$ to 18 before normalizing and k represents each individual response; $\max S_i(k)$ represents the highest value of each response k and $\min S_i(k)$ represents the lowest value of each response k. On the other side, $y_i(k)$ is the normalized value of responses in each experimental run.

Stage II (Computing Grey Relational Coefficient (GRC)): Then, GRC calculation is made for each experimental run using the following equation.

$$\text{GRC} = \omega_i(k) = \frac{\Delta\min + \xi \cdot \Delta\max}{\Delta 0_i(k) + \xi \cdot \Delta\max}, \tag{4}$$

where $\omega_i(k)$ represents the GRC value of each response at each experimental run i, and ξ is the distinguishing coefficient which is assumed 0.5 [29]. $\Delta 0_i(k) = |y_0(k) - y_i(k)|$ represents the deviation sequence. $\Delta\max$ is the largest value of $\Delta 0_i(k)$ and $\Delta\min$ is the smallest value of $\Delta 0_i(k)$ which are computed by the following formulas, sequentially:

$$\Delta\max = \max_{i,k} \Delta 0_i(k), \tag{5}$$

$$\Delta\min = \min_{i,k} \Delta 0_i(k). \tag{6}$$

Stage III (Determining Grey Relational Grade (GRG)): Finally, GRG value is made by multiplying the relative weight value (w_k) by the computed GRC as follows:

$$\gamma_i(\text{GRG}) = \sum_{k=1}^{n} w_k \cdot \omega_i(k). \tag{7}$$

In this study, the relative weight value (w_k) of each response has been calculated using the principal component analysis (PCA). The principal component analysis (PCA) was introduced by Pearson [30] and Hotelling [31] for explaining the structure of variance covariance matrix in a linear way. The detailed stepwise procedure of incorporating principal component analysis (PCA) with Taguchi-GRA is discussed below:

Step 1: Development a new variance covariance matrix (W) of multiple quality characteristics as follows:

$$W = \begin{bmatrix} \omega_1(1) & \omega_1(2) & \dots & \omega_1(n) \\ \omega_2(1) & \omega_2(2) & \dots & \omega_2(n) \\ \dots & \dots & \dots & \dots \\ \omega_m(1) & \omega_m(2) & \dots & \omega_m(n) \end{bmatrix}; \quad i = 1, 2, \dots, m; \quad p = 1, 2, \dots, n, \tag{8}$$

where m is the number of experimental runs, n is the number of responses and ω is the grey relational coefficient of each response. In this study, $m = 18$ and $n = 3$. Then the correlation coefficient array can be evaluated as follows:

$$r_{pq} = \frac{\operatorname{cov}\left(\omega_i(p), \omega_i(q)\right)}{\partial_{\omega_i(p)} \times \partial_{\omega_i(q)}}, \tag{9}$$

where $\operatorname{cov}(\omega_i(p), \omega_i(q))$ represents the covariance of the sequence $\omega_i(p)$ and $\omega_i(q) \cdot \partial_{\omega_i(p)}$ is the standard deviation of $\omega_i(p)$ and $\partial_{\omega_i(q)}$ is the standard deviation of $\omega_i(q)$.

Step 2: Determining the eigenvalues and eigenvectors from the correlation coefficient array using the following equation.

$$(r - \lambda_k I_m)\, V_{ik} = 0, \tag{10}$$

where λ_k represents numerical eigenvalues, $\sum_{k=1}^{n} \lambda_k = n$; $k = 1, 2, \dots, n$; $V_{ik} = [a_{(k,1)} \quad a_{(k,2)} \quad \dots \quad a_{(k,n)}]^T$ represents the eigenvectors corresponding to the eigenvalues λ_k.

Step 3: Then, computing the principal components using the following equation.

$$C_{mk} = \sum_{i=1}^{n} x_m(i) \cdot V_{ik}, \tag{11}$$

where C_{m1} is the first principal component, C_{m2} is the second principal component and so on.

Step 4: Because the first principal component describes the highest variance of the process [19], this value is used for further processing. Finally, the squared value of first principal component is considered as the relative weight value (w_k) of each response.

3.2.2. Modified weighted Technique for Order Preference by Similarity to Ideal Solution (TOPSIS)

TOPSIS was developed by Hwang and Yoon in 1981 as a multi-criteria decision analysis (MCDA) method. At the former stage, the basic concept was that the chosen alternative represents the smallest geometrical distance from the positive

ideal solution and the longest distance from the negative ideal solutions. Using an appropriate algorithm, this technique selects the optimum alternative which means the smallest distance from the positive ideal solution and the farthest distance from the negative ideal solution. In TOPSIS, a trade-off is made between the criteria in which poor result of one criterion is counterbalanced by a better result in another criterion, so this technique can be considered as a realistic way of decision making. The stepwise procedure is given below in detail:

Step 1: To create a decision matrix consisting of m alternatives and n attributes with their intersection symbolized as $(A_{ij})_{m\times n}$. Here, $m = 18$, $n = 3$ and the formulated matrix can be expressed as follows:

$$(A_{ij})_{m\times n} = \begin{bmatrix} A_{11} & A_{12} & \dots & A_{1n} \\ A_{21} & A_{22} & \dots & A_{2n} \\ \dots & \dots & \dots & \dots \\ A_{m1} & A_{m2} & \dots & A_{mn} \end{bmatrix}; \quad i = 1, 2, \dots, m \text{ and } j = 1, 2, \dots, n. \tag{12}$$

Step 2: To convert matrix $(A_{ij})_{m\times n}$ into normalized matrix R_{ij} using the following formula:

$$R_{ij} = \frac{A_{ij}}{\sqrt{\sum_{i=1}^{m} A_{ij}^2}}. \tag{13}$$

Step 3: To measure the individual weight of each attribute using the following equation without the influence of decision maker's preference value.

$$\delta_j = \frac{\sigma_j}{\sum_{k=1}^{n} \sigma_k}. \tag{14}$$

Next step is to multiply this weight value by the normalized matrix R_{ij} for formulating a weighted normalized matrix $N = \vartheta_{ij}$.

$$N = \delta_j \times R_{ij}; \qquad \sum_{j=1}^{n} \delta_j = 1. \tag{15}$$

Step 4: To find out the best solution and the worst solution.

Best solution:

$$\begin{aligned} \mathrm{Sol}^+ &= \{\max_i \vartheta_{ij} |\ j \in J,\ \min_i \vartheta_{ij} |\ j \in J';\ i = 1, 2, \dots m\} \\ &= \{\vartheta_1^+, \vartheta_2^+, \dots, \vartheta_n^+\}. \end{aligned} \tag{16}$$

Worst solution:

$$\begin{aligned} \mathrm{Sol}^- &= \{\min_i \vartheta_{ij} |\ j \in J,\ \max_i \vartheta_{ij} |\ j \in J';\ i = 1, 2, \dots m\} \\ &= \{\vartheta_1^-, \vartheta_2^-, \dots, \vartheta_n^-\}. \end{aligned} \tag{17}$$

Sol^+ symbolizes the positive ideal solutions and Sol^- defines the negative ideal solutions.

Step 5: To calculate distance measures using n-dimensional Euclidean distance formula expressed as:

$$d_i^+ = \sqrt{\sum_{j=1}^{n} (\vartheta_{ij} - S_j^+)^2}\,; \quad i = 1, 2, \ldots, m, \tag{18}$$

$$d_i^- = \sqrt{\sum_{j=1}^{n} (\vartheta_{ij} - S_j^-)^2}\,; \quad i = 1, 2, \ldots, m. \tag{19}$$

For any response, d_i^+ is the calculated best distance from Sol^+ value and d_i^- is the calculated worst distance from Sol^- value [24].

Step 6: The final step is to compute closeness coefficients (coeff_i^+) to the ideal solutions and to provide appropriate ranks for each alternative according to their relative closeness coefficients (coeff_i^+).

$$\mathrm{coeff}_i^+ = \frac{d_i^-}{d_i^+ + d_i^-}\,. \tag{20}$$

4. Results and discussions

All the aforementioned measured and computed responses are listed in Table 5 with their corresponding (S/N) ratios which are calculated using Eq. (3). Calculations are facilitated by MINITAB 17 statistical software package. Then, the mean influence of input parameters on each response is graphically depicted in Fig. 3 and the highest point in the graph represents the optimal level of an individual factor [19].

Cutting speed ranges from 85 m/min to 144 m/min, and it has remarkable effects on θ, R_a and E_{sp}. One can notice easily from Fig. 3a that θ has an increasing tendency with rising level of V_c because of excess heat generation in the cutting vicinity. In this study, R_a and E_{sp} decrease very sharply with increasing V_c due to thermal softening of the work specimen at high heat generation, which has also been reported previously [32]. This accelerates the smooth cutting with minimum surface damage and less energy. From Fig. 3c one can notice that the cutting speed is the most dominating factors for changing specific cutting energy, this fact is also confirmed by a previous analysis report [32].

Like V_c, feed rate has also a significant influence on each response. At higher S_0, material removal volume increases, which results in immense heat formation in the cutting area [19]. R_a increases at a high level of S_0 due to extensive formation of feed marks on the machined surface for larger chip load, which is in agreement with other research results [19]. Actually, for the work specimen being softer due to immense heat at a high level of feed rate, a lower force is needed, in the result

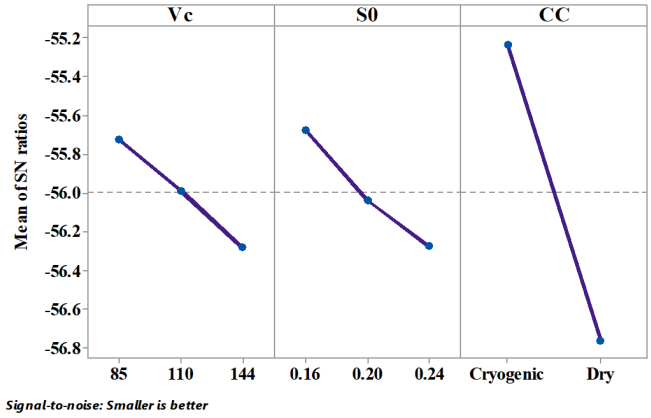

(a)

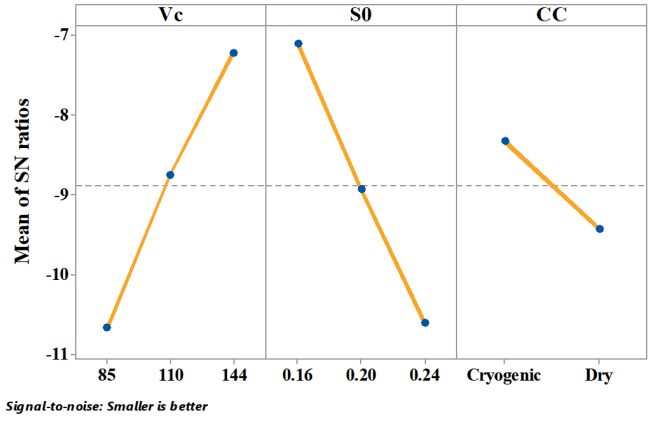

(b)

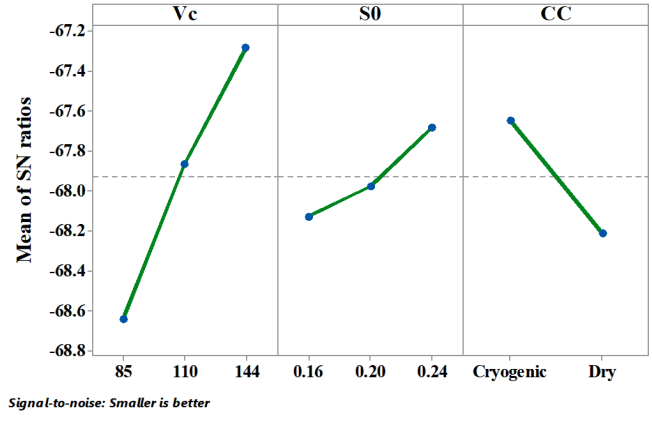

(c)

Fig. 3. Main effect plot of (S/N) ratios of (a) θ; (b) R_a and (c) E_{sp}

Table 5.
Experimentally measured and computed responses with their corresponding (S/N) ratios

Experimental runs	Responses			(S/N) ratios of		
	θ, °	R_a, µm	E_{sp}, N/mm^2	θ, dB	R_a dB	E_{sp}, dB
1.	654	3.02	2991.67	−56.3116	−9.6001	−69.5183
2.	672	3.80	2850.00	−56.5474	−11.5957	−69.0969
3.	693	4.46	2772.22	−56.8147	−12.9867	−68.8566
4.	667	2.40	2616.67	−56.4825	−7.6042	−68.3550
5.	687	2.89	2520.00	−56.7391	−9.2180	−68.0280
6.	711	3.54	2466.67	−57.0374	−10.9801	−67.8422
7.	680	2.00	2350.00	−56.6502	−6.0206	−67.4214
8.	706	2.40	2383.30	−56.9761	−7.6042	−67.5436
9.	733	2.92	2305.56	−57.3021	−9.3077	−67.2555
10.	527	2.53	2716.67	−54.4362	−8.0624	−68.6807
11.	563	3.21	2526.67	−55.0102	−10.1301	−68.0510
12.	576	3.85	2416.67	−55.2084	−11.7092	−67.6643
13.	555	2.05	2441.67	−54.8859	−6.2351	−67.7537
14.	584	2.58	2453.33	−55.3283	−8.2324	−67.7951
15.	592	3.25	2350.00	−55.4464	−10.2377	−67.4214
16.	582	1.80	2250.00	−55.2985	−5.1055	−67.0437
17.	604	2.20	2333.33	−55.6207	−6.8485	−67.3595
18.	620	2.65	2255.56	−55.8478	−8.4649	−67.0651

of which energy consumption rate is reduced [33]. As far as surface roughness is concerned, the feed rate is observed as the most significant factors in Fig. 3b that again coincides with another research results [32].

In this analysis, dry and cryogenic cooling was applied in the cutting environments. All the selected responses θ, R_a and E_{sp} decrease in cryogenic cooling (according to Fig. 3), which confirms the effectiveness of cooling and lubrication property of the used cryogenic cooling method. θ is drastically reduced in cryogenic cooling because of lower working temperature of LN_2 (−196°C) which evacuates heat from the cutting zone [34]. Lubrication effect of LN_2 helps to reduce friction [35] between tool-work interfaces, so a smoother surface is achieved and lower specific cutting energy is required in cryogenic cooling.

In summary, it can be mentioned that maximum chip tool temperature at lower speed (85 m/min) with lower feed rate (0.16 mm/rev) under cryogenic cooling is reduced compared to that in dry turning. But, minimum surface roughness is observed at the higher speed (144 m/min) with the lower feed rate (0.16 mm/rev)

under cryogenic cooling and finally, specific cutting energy requirement is reduced at the higher speed (144 m/min) with the higher feed rate (0.24 mm/rev) under cryogenic cooling. The significance of input factors is different in terms of the three responses and, moreover, the desirable response values are found at different levels of input factors. These facts encouraged the authors to move towards multi-response optimization. Besides, in this experiment, tool wear was also checked out for both cutting condition at 135 m/min cutting speed, 0.2 mm/rev feed rate and 1.5 mm depth of cut depicted in Fig. 4. In cryogenic cooling, the growth rate of flank wear was found uniform and slower than that in dry turning, which might be due to the positive impact of extreme cooling by liquid nitrogen at work-tool interface. Conversely, notch wear was also minimized in cryogenic cooling which prevents the sudden breakage of tool, reduces cutting force requirements and as a whole improves process reliability with lowering tool cost. The span of tool life was also increased under cryogenic cooling (50 min), compared to only 35 min in dry turning. But, after 45 min machining, chipping was noticed in cutting edges, which was assumed the result of non-uniform cooling by cryogen due to improper penetration into some intricate regions.

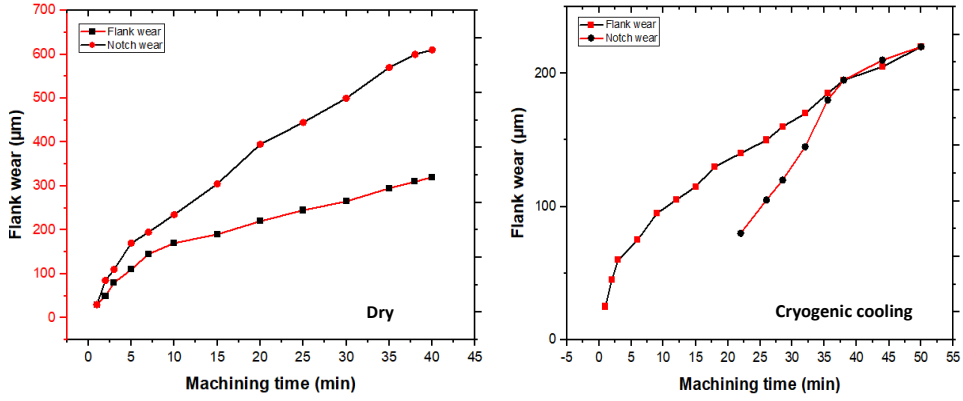

(a) (b)

Fig. 4. Growth rate of tool wear under (a) dry and (b) cryogenic cooling

4.1. Coupling hybrid GRA-PCA with Taguchi for multi-response optimization

Normalized values, deviation sequences and Grey relational coefficients (GRCs) of the corresponding responses are determined using Eqs. (3), (4) and are listed in Table 6. Next, the relative weights of each response are computed on PCA using MINITAB 17. Initially, the eigenvalues with their explained variations are calculated and afterwards the eigenvectors related to these eigenvalues are computed, as it is listed in Table 7. Finally, the grey relational grades (GRGs)

Table 6.

Normalized values, deviational sequences and GRC for responses

Experimental runs	Normalized values			Deviational sequences			GRC		
	θ	R_a	E_{sp}	θ	R_a	E_{sp}	θ	R_a	E_{sp}
1.	0.3456	0.4297	0.0000	0.6544	0.5703	1.0000	0.4331	0.4672	0.3333
2.	0.2633	0.1765	0.1703	0.7367	0.8235	0.8297	0.4043	0.3778	0.3760
3.	0.1701	0.0000	0.2674	0.8299	1.0000	0.7326	0.3760	0.3333	0.4056
4.	0.2860	0.6830	0.4701	0.714	0.3170	0.5299	0.4119	0.6120	0.4855
5.	0.1964	0.4782	0.6022	0.8036	0.5218	0.3978	0.3836	0.4893	0.5569
6.	0.0924	0.2546	0.6773	0.9076	0.7454	0.3227	0.3552	0.4015	0.6078
7.	0.2275	0.8839	0.8474	0.7725	0.1161	0.1526	0.3929	0.8116	0.7662
8.	0.1138	0.6830	0.7980	0.8862	0.3170	0.2020	0.3607	0.6120	0.7123
9.	0.0000	0.4668	0.9146	1.0000	0.5332	0.0854	0.3333	0.4839	0.8541
10.	1.0000	0.6248	0.3385	0.0000	0.3752	0.6615	1.0000	0.5713	0.4305
11.	0.7997	0.3625	0.5929	0.2003	0.6375	0.4071	0.7140	0.4396	0.5512
12.	0.7306	0.1621	0.7492	0.2694	0.8379	0.2508	0.6499	0.3737	0.6660
13.	0.8431	0.8567	0.7131	0.1569	0.1433	0.2869	0.7612	0.7772	0.6354
14.	0.6887	0.6032	0.6964	0.3113	0.3968	0.3036	0.6163	0.5575	0.6222
15.	0.6475	0.3488	0.8474	0.3525	0.6512	0.1526	0.5865	0.4343	0.7662
16.	0.6991	1.0000	1.0000	0.3009	0.0000	0.0000	0.6242	1.0000	1.0000
17.	0.5867	0.7788	0.8724	0.4133	0.2212	0.1276	0.5475	0.6933	0.7967
18.	0.5074	0.5737	0.9914	0.4926	0.4263	0.0086	0.5037	0.5398	0.9831

Table 7.

Eigenvalues and explained variation

Principal component	Eigenvalues	Variations (%)	Eigenvectors		
			θ	R_a	E_{sp}
Pc_1	1.5663	52.20	0.248	0.713	0.656
Pc_2	1.0190	34.00	0.923	0.033	−0.384
Pc_3	0.4147	13.80	−0.295	−0.701	−0.649
		Relative weights	0.062	0.508	0.430

for all experimental runs are calculated using Eq. (7) and contained with their corresponding ranks in Table 8.

In order to achieve the desired goal, the maximum GRG is selected, which appears at experimental run no. 16 corresponding to the highest level of speed (144 m/min) with the lowest level of feed rate(0.16 mm/rev) under cryogenic cool-

Table 8.

Grey relational grades (GRG) for 18 comparability sequences

Experimental runs	GRG	Rank	Experimental runs	GRG	Rank	Experimental runs	GRG	Rank
1.	0.4075	**16**	7.	0.7661	**2**	13.	0.7152	**5**
2.	0.3787	**17**	8.	0.6395	**6**	14.	0.5890	**8**
3.	0.3670	**18**	9.	0.6337	**7**	15.	0.5865	**9**
4.	0.5452	**10**	10.	0.5373	**11**	16.	0.9767	**1**
5.	0.5118	**13**	11.	0.5046	**14**	17.	0.7287	**3**
6.	0.4873	**15**	12.	0.5165	**12**	18.	0.7282	**4**

ing. It can be deduced from the mean response Table 9 that the cutting speed, followed by the cutting condition and the feed rate, noticeably overwhelm the mean GRG. According to the main effect plot in Fig. 5a, the optimal input factors for highest GRG can be symbolically presented as $V_c 3 S_0 1 CC2$. This results are then reconfirmed by ANOVA at 95% confidence level, which is given in Table 10. It can be concluded from ANOVA table that all the selected input process variables are statistically significant, because the calculated P-values of all input factors are less than 0.05. Moreover, the proposed model is also statistically significant because its P-value is much lower than 0.05. Cutting velocity, having 65.19% contribution, is the most important factor for maximizing the GRG value. Then, the cutting condition is the second most influential process variable having 18.20%, and the feed rate is found the third influential input factor (10.42% contribution). The percentage contribution of error is found 6.19% which indicates the high acceptability of the proposed technique with the obtained results [36].

Table 9.

Average GRG values at various levels of input factors

Factors	Level 1	Level 2	Level 3	Max–Min	Rank
V_c	0.4519	0.5725	**0.7455**	0.2936	1
S_0	**0.6580**	0.5587	0.5532	0.1048	3
CC	0.5263	**0.6536**	–	0.1273	2

Bold numbers containing levels denote the optimum level of input variables.

Moreover, the correlations are explained with the help of interaction plot and one can see easily the combined effect of input factors on responses. From Fig. 5b, it can be easily noticed that there is a strong interaction between cutting speed and feed because non-parallel line depicts the greater correlation between the two factors for changing a response. In a similar manner, parallel lines between cutting speed and cutting condition, as well as feed rate and cutting condition, denote the poor correlation between the mentioned input factors.

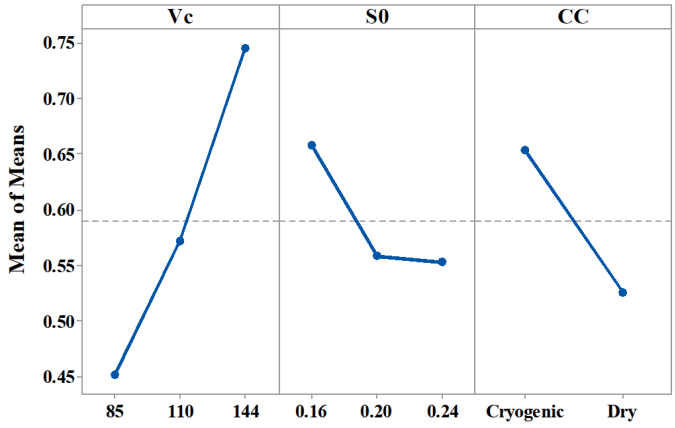

(a)

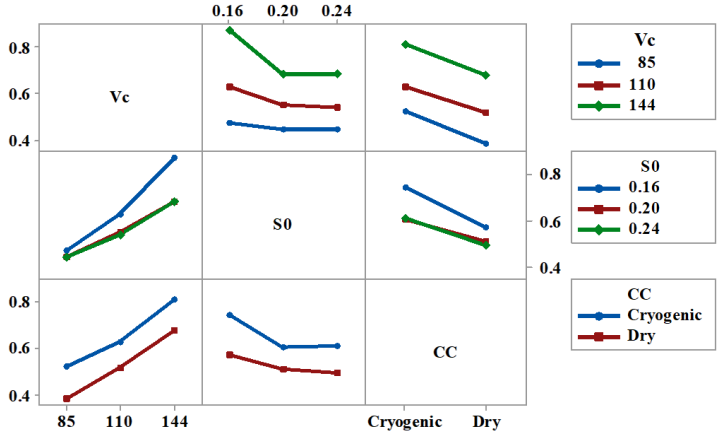

(b)

Fig. 5. (a) Main effects plot of average grey relational grade (GRG); (b) Interaction plot of GRG

Table 10.

ANOVA using general linear model (within 95% confidence level) for average GRG with percent contribution (here, SS – sum of squares, MS – mean squares, DoF – degrees of freedom)

Source	DoF	SS	MS	F-ratio	P-value	% contribution
Model	5	0.75161	0.07413	36.33	0.00001	93.81
V_c	2	0.26126	0.130631	63.19	0.0000	65.19
S_0	2	0.04174	0.020871	10.10	0.0030	10.42
CC	1	0.07295	0.072949	35.29	0.0000	18.20
Error (e)	12	0.02481	0.002067	–	–	6.19
Total	17	0.40076	–	–	–	100

Here $R - sq = 93.81\%$.

In the regression analysis, cutting condition is the only categorical factor having two different levels: dry and cryogenic cooling. For each cutting condition, a separate equation is generated, as it is numerically presented in following equations, sequentially.

$$\text{GRG}\,(V_c,\ S_0,\ \text{Dry}) = 0.2254 + 0.004982V_c - 1.310S_0\,, \tag{21}$$

$$\text{GRG}\,(V_c,\ S_0,\ \text{Cryogenic}) = 0.3527 + 0.004982V_c - 1.310S_0\,. \tag{22}$$

From mathematical analysis of both equations it is found that the only difference between these equations is their intercept value. Equation (22) manifests that turning under cryogenic cooling is able to provide results at least 56.60% better than dry turning, which again proves the effectiveness of cryogenic cooling in turning AISI 1040 steel. The consistency between GRG values predicted using regression model and experimental GRG values is shown in Fig. 6. Notice that the predicted values fit well the experimental ones, which confirms the suitability of this model for prediction of response variables in the defined situation.

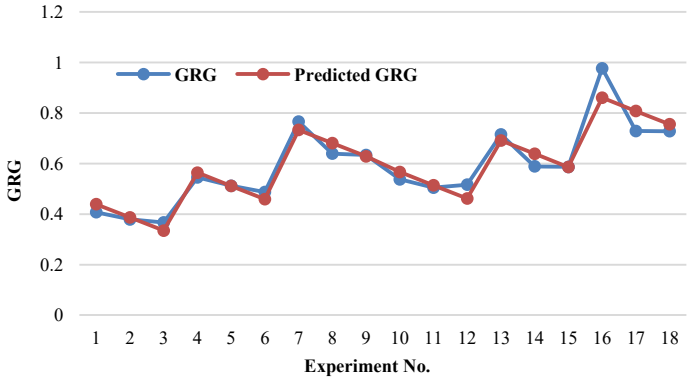

Fig. 6. Experimental and predicted values of GRG using linear regression

4.1.1. Predicting the optimum value of GRG and validation tests

The predicted optimum value of grey relational grade at optimal parameter settings has been computed using following equation.

$$\rho_{\text{GRG}} = \bar{\rho}_{\text{GRG}} + \left(\bar{V}_{c\,\text{opt}} - \bar{\rho}_{\text{GRG}}\right) + \left(\bar{S}_{0\,\text{opt}} - \bar{\rho}_{\text{GRG}}\right) + \left(\overline{\text{CC}}_{\text{opt}} - \bar{\rho}_{\text{GRG}}\right). \tag{23}$$

Here ρ_{GRG} denotes the optimum predicted value of GRG and $\bar{\rho}_{\text{GRG}}$ is the mean value of GRG for a total of 18 experimental trials. $\bar{V}_{c\,\text{opt}}$ represents the mean value of GRG at optimal level of cutting speed when other input parameters may vary similarly, $\bar{S}_{0\,\text{opt}}$ and $\overline{\text{CC}}_{\text{opt}}$ carry out the mean value of GRG at optimal level of feed rate and cutting condition. The predicted mean GRG value is found 0.8772 using

Eq. (23) in Table 11 and the previously achieved experimental GRG value is 0.9767. This clearly indicates that the experimental result is 10.19% better than the predicted optimum result. So, it can be concluded that this hybrid optimization technique has successfully provided the solution of multi-response optimization problem with minimizing temperature, surface roughness and specific cutting energy.

Table 11.

Results of validation tests for mean GRC

	Initial parameter	Optimal parameter	
		Experimental value	Predicted value
Level	$V_{c1} - S_{01} - \mathrm{CC}_1$	$V_{c3} - S_{01} - \mathrm{CC}_2$	$V_{c3} - S_{01} - \mathrm{CC}_2$
Mean GRG	0.3456	0.9767	0.8772

The subscript number of each input parameter represents the corresponding level.

4.2. Coupling modified weighted TOPSIS with Taguchi for optimization

As far as the methodology discussed in previous section is concerned, the normalized (S/N) values are calculated using Eq. (13). Then, the relative weights of responses are determined using Eq. (14) and putting these weights into Eq. (15) one computes the weighted normalized (S/N) value. All the calculated normalized (S/N) values and weighted normalized (S/N) values are listed in Table 12.

Afterwards, the positive ideal (best) solutions (Sol^+) and negative ideal (worst) solutions (Sol^-) are defined by applying Eqs. (16) and (17) finally, by putting those values into Eqs. (18) and (19), one measures the distance from Sol^+ to Sol^-. The closeness coefficients are shown in Table 13 with their corresponding ranks. The experimental run order with the largest value of closeness coefficient is generally selected as the optimum condition [37]. It was found that the optimal turning performance was obtained at experimental run order 16 (cutting speed 144 m/min (level 3) feed rate 0.16 mm/rev (level 1) and cryogenic cooling (level 2), which agreed with previous results of hybrid Taguchi-GRA-PCA. The mean response of closeness coefficients is given in Table 14 and graphically presented in Fig. 7a. The highest (max–min) value is found for the feed rate (rank 1) that is a little bit greater than the cutting speed (rank 2) and the cutting condition has the least influence (rank 3). Fig. 7b represents the interaction plot of input factors and closeness coefficients.

Similarly as in the case of previous results from Taguchi-GRA-PCA, it has been proven that cryogenic cooling is more effective than dry turning due to higher intercept value in the second of following equations.

$$\mathrm{coeff}_i^+ \,(V_c,\, S_0,\, \mathrm{Dry}) = 0.7356 + 0.007324 V_c - 5.562 S_0\,, \tag{24}$$

$$\mathrm{coeff}_i^+ \,(V_c,\, S_0,\, \mathrm{Cryogenic}) = 0.8748 + 0.007324 V_c - 5.562 S_0\,. \tag{25}$$

Table 12.

Calculated normalized and weighted normalized (S/N) ratios of all responses

Experimental runs	Normalized (S/N) ratios of			Weighted normalized (S/N) ratios of			Distance measures	
	θ	R_a	E_{sp}	θ	R_a	E_{sp}	d_i^+	d_i^-
1.	−0.23700	−0.24786	−0.24120	−0.01396	−0.22334	−0.00965	0.1046	0.0788
2.	−0.23799	−0.29938	−0.23974	−0.01402	−0.26976	−0.00959	0.1509	0.0324
3.	−0.23912	−0.33530	−0.23890	−0.01409	−0.30213	−0.00956	0.1834	0.0002
4.	−0.23772	−0.19633	−0.23716	−0.01401	−0.17691	−0.00949	0.0581	0.1252
5.	−0.23880	−0.23800	−0.23603	−0.01407	−0.21445	−0.00944	0.0957	0.0877
6.	−0.24006	−0.28349	−0.23538	−0.01414	−0.25544	−0.00942	0.1367	0.0467
7.	−0.23843	−0.15544	−0.23392	−0.01405	−0.14006	−0.00936	0.0213	0.1621
8.	−0.23980	−0.19633	−0.23435	−0.01413	−0.17691	−0.00938	0.0581	0.1252
9.	−0.24117	−0.24031	−0.23335	−0.01421	−0.21654	−0.00934	0.0978	0.0856
10.	−0.22911	−0.20816	−0.23829	−0.01350	−0.18757	−0.00953	0.0687	0.1146
11.	−0.23152	−0.26155	−0.23611	−0.01364	−0.23567	−0.00945	0.1169	0.0665
12.	−0.23236	−0.30232	−0.23477	−0.01369	−0.27241	−0.00939	0.1536	0.0297
13.	−0.23100	−0.16098	−0.23508	−0.01361	−0.14505	−0.00941	0.0263	0.1571
14.	−0.23286	−0.21255	−0.23522	−0.01372	−0.19152	−0.00941	0.0727	0.1106
15.	−0.23336	−0.26432	−0.23392	−0.01375	−0.23817	−0.00936	0.1194	0.0639
16.	−0.23274	−0.13182	−0.23261	−0.01371	−0.11878	−0.00930	0.0002	0.1834
17.	−0.23409	−0.17682	−0.23371	−0.01379	−0.15933	−0.00935	0.0406	0.1428
18.	−0.23505	−0.21855	−0.23269	−0.01385	−0.19693	−0.00931	0.0782	0.1052

The relative weight value of temperature, surface roughness and specific cutting energy are:
$w_\theta = 0.058918$; $w_{R_a} = 0.901070$; $w_{E_{sp}} = 0.040013$.
Here, $\text{Sol}^+ = -0.01350, -0.11878, -0.0002$; $\text{Sol}^- = -0.01421, -0.30213, -0.00965$.

Table 13.

Computation of distance measures, closeness coefficients and ranking of alternatives (bold numbers denote rank)

Experimental run	coeff$_i^+$	Rank	Experimental run	coeff$_i^+$	Rank	Experimental run	coeff$_i^+$	Rank
1.	0.4297	**12**	7.	0.8839	**2**	13.	0.8567	**3**
2.	0.1765	**16**	8.	0.6829	**6**	14.	0.6033	**8**
3.	0.0008	**18**	9.	0.4668	**11**	15.	0.3488	**14**
4.	0.6829	**5**	10.	0.6248	**7**	16.	0.9989	**1**
5.	0.4782	**10**	11.	0.3625	**13**	17.	0.7788	**4**
6.	0.2547	**15**	12.	0.1621	**17**	18.	0.5738	**9**

Table 14.

Mean response table of closeness coefficients

Factors	Level 1	Level 2	Level 3	Max–Min	Rank
V_c	0.2928	0.5374	**0.7309**	0.4400	2
S_0	**0.7462**	0.5137	0.3012	0.4450	1
CC	0.4507	**0.5900**	–	0.1392	3

Bold numbers containing levels denote the optimum level of input variables.

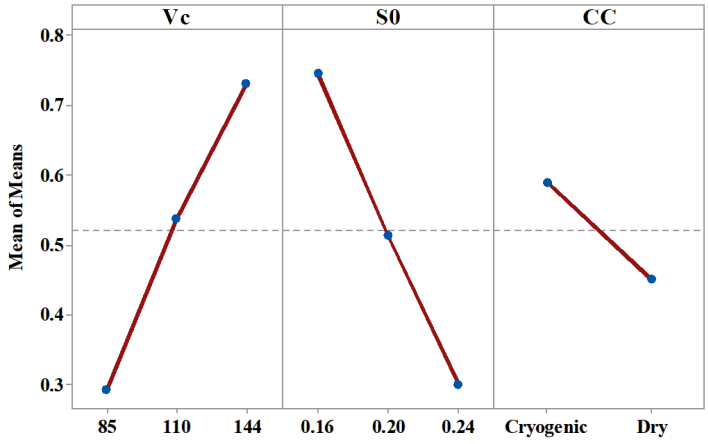

(a)

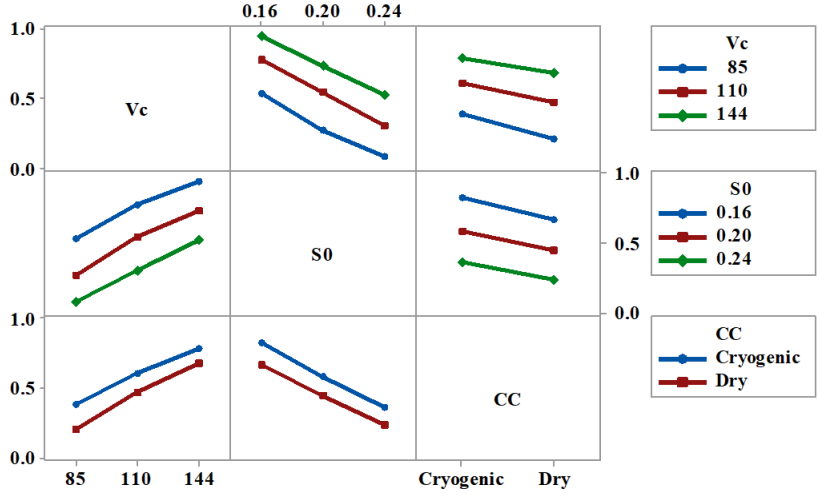

(b)

Fig. 7. (a) Main effects plot of average closeness coefficients; (b) Interaction plot of showing the effect of input parameters on closeness coefficients

Table 15.
ANOVA using general linear model (within 95% confidence level) for closeness coefficients (here, SS – sum of squares, MS – mean squares, DoF – degrees of freedom)

Source	DoF	SS	MS	F-ratio	P-value	% contribution
Model	5	1.26012	0.2520	346.6	0.0000	99.30
V_c	2	0.57842	0.2892	397.9	0.0000	45.58
S_0	2	0.59445	0.2972	408.9	0.0000	46.85
CC	1	0.08725	0.0872	120.04	0.0000	6.87
Error (e)	12	0.00872	0.0007	–	–	0.70
Total	17	1.26885	–	–	–	

Here, $R - sq = 0.9931$.

One can easily notice that the experimental and predicted values fit very well, which proves the applicability of this model for predicting the response variables in turning of AISI 1040 steel (Fig. 8).

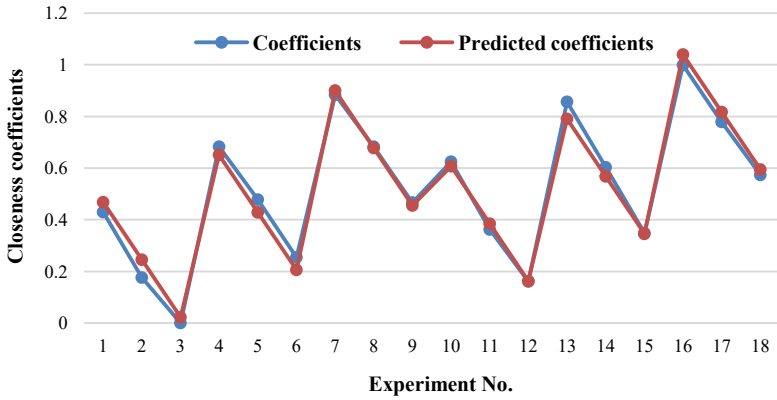

Fig. 8. Experimental and predicted values of closeness coefficients using linear regression

4.2.1. Predicting the optimum value of closeness coefficient at optimal parameter settings and validation tests

The prediction of optimum value of closeness coefficient at optimal parameter settings has been done using the following equation.

$$\rho_{\text{coeff}_i^+} = \bar{\rho}_{\text{coeff}_i^+} + \left(\bar{V}_{c\,\text{opt}} - \bar{\rho}_{\text{coeff}_i^+}\right) + \left(\bar{S}_{0\,\text{opt}} - \bar{\rho}_{\text{coeff}_i^+}\right) + \left(\overline{\text{CC}}_{\text{opt}} - \bar{\rho}_{\text{coeff}_i^+}\right). \quad (26)$$

Here $\rho_{\text{coeff}_i^+}$ denotes the optimum predicted value of closeness coefficient and $\bar{\rho}_{\text{coeff}_i^+}$ is the mean value of closeness coefficients for a total of 18 experimental trials. $\bar{V}_{c\,\text{opt}}$ represents the mean value of closeness coefficients at optimal level of cutting speed when other input parameters may vary similarly $\bar{S}_{0\,\text{opt}}$ and $\overline{\text{CC}}_{\text{opt}}$

carry out the mean value of closeness coefficients at optimal level of feed rate and cutting condition. Three more experimental trials were performed in optimal parameter setting for validating the model. The experimental and predicted mean closeness coefficient values are 0.9986 and 0.9993, as shown in Table 16. The predicted result is 0.07% better than the predicted optimum result, which denotes the higher accuracy of this proposed optimization technique with lower error rate.

Table 16.

Results of validation tests for mean closeness coefficients

	Initial parameter	Optimal parameter	
		Experimental value	Predicted value
Level	$V_{c1} - S_{01} - CC_1$	$V_{c4} - S_{01} - CC_2$	$V_{c4} - S_{01} - CC_2$
Mean closeness coefficients	0.429722	0.9986	0.9993

The subscript number of each input parameter represents the corresponding level.

4.3. Comparison of results achieved by two MCDM techniques

In this subsection, we compare the results obtained by two different multi-criteria decision making (MCDM) techniques in terms of ranking different alternatives. From Table 17, one can easily notice that in both optimization techniques the experiment number 16 provides the optimum result within the boundary conditions. Both optimization techniques provide good optimum results, but one can see that accuracy of prediction is higher in Taguchi integrated modified weighted TOPSIS, which has been already discussed in the previous subsection 4.2.1.

Table 17.

Comparative results in hybrid Taguchi-GRA-PCA and Taguchi integrated modified weighted TOPSIS for optimization (bold numbers represent rank)

Experiment run	Rank by		Experiment run	Rank by	
	Hybrid Taguchi-GRA-PCA	Taguchi with modified weighted TOPSIS		Hybrid Taguchi-GRA-PCA	Taguchi with modified weighted TOPSIS
1.	**16**	**12**	10.	**11**	**7**
2.	**17**	**16**	11.	**14**	**13**
3.	**18**	**18**	12.	**12**	**17**
4.	**10**	**5**	13.	**5**	**2**
5.	**13**	**10**	14.	**8**	**8**
6.	**15**	**15**	15.	**9**	**14**
7.	**2**	**2**	16.	**1**	**1**
8.	**6**	**6**	17.	**3**	**4**
9.	**7**	**11**	18.	**4**	**9**

5. Conclusions

This paper evaluates the effect of turning process parameters: cutting speed, feed rate and cutting condition on machining capability taking into account chip-tool interface temperature, surface roughness and specific cutting energy in turning AISI 1040 steel through experimentation. In addition, two different Multi-Criteria Decision Making techniques, i.e., hybrid Taguchi-GRA-PCA and modified weighted TOPSIS integrated with Taguchi were applied for optimization. ANOVA and regression models were developed for identifying the significant input factors and for accurate mathematical prediction of the responses. Validation tests were performed at optimal settings of input parameters for declaring the validity of the proposed models. Now, the outcomes can be summed up as follows:

1. Cryogenic cooling improves surface finish as well as reduces chip tool interface temperature and specific cutting energy better than dry turning.
2. Hybrid Taguchi-GRA-PCA and modified weighted TOPSIS integrated with Taguchi are very easy and simple ways of multi-response optimization. The grey relational grade (GRG) is the indicator's single key of multiple responses in hybrid Taguchi-GRA-PCA and the closeness coefficient is the representative of multi-response performance index (MRPI) in the modified weighted TOPSIS integrated with Taguchi. The predicted optimal parameters settings are the same for both optimization methods and those are the following: cutting speed 144 m/min (level 3), feed rate 0.16 mm/rev (level 1) and cutting condition (cryogenic cooling, level 2).
3. ANOVA also manifested that the both models are significant within 95% confidence level. The cutting speed exerts the most notable impacts on GRG and the feed rate has the highest influence on the closeness coefficient.
4. Using the simple linear regression for both models, one observed that the predicted values fit well the corresponding experimental values. However, the prediction accuracy of Taguchi integrated modified weighted TOPSIS is found higher than that of hybrid Taguchi-GRA-PCA. Moreover, the advantage of cryogenic cooling-assisted turning over dry turning in terms of efficiency has been proven experimentally as well as mathematically in regression equation.

The prediction results highlighted the better performance of the modified weighted TOPSIS integrated with Taguchi compared to the hybrid Taguchi-GRA-PCA in terms of optimization. It is expected that both of these optimization techniques will be helpful for future practitioners, manufacturers and researchers in problem solving area. But, in the present work material removal rate (MRR), chip morphology and wear profile have not been analysed. This can be carried out in future using both coated and uncoated cutting inserts in future for attaining a better robustness of turning AISI 1040 steel under LN_2 assisted cryogenic cooling.

Acknowledgements

We sincerely thank honourable editors and reviewers for constructive comments which led to serious improvement of the article.

Manuscript received by Editorial Board, April 23, 2020;
final version, October 20, 2020.

References

[1] S.S. Nair, T. Ramkumar, M. Selva Kumar, and F. Netto. Experimental investigation of dry turning of AISI 1040 steel with TiN coated insert. *Engineering Research Express*, 1(2):1–13, 2019. doi: 10.1088/2631-8695/ab58d9.

[2] M.N. Sultana, N.R. Dhar, and P.B. Zaman. A Review on different cooling/lubrication techniques in metal cutting. *American Journal of Mechanics and Applications*, 7(4):71–87, 2019. doi: 10.11648/j.ajma.20190704.11.

[3] M.N. Sultana, P.B. Zaman, and N.R. Dhar. GRA-PCA coupled with Taguchi for optimization of inputs in turning under cryogenic cooling for AISI 4140 steel. *Journal of Production Systems & Manufacturing Science*, 1(2):40–62, 2020.

[4] M. Mia. Multi-response optimization of end milling parameters under through-tool cryogenic cooling condition. *Measurement*, 111:134–145, 2017. doi: 10.1016/j.measurement.2017.07.033.

[5] L.S. Ahmed, N. Govindaraju, and M. Pradeep Kumar. Experimental investigations on cryogenic cooling in the drilling of titanium alloy. *Materials and Manufacturing Processes*, 31(5):603–607, 2016. doi: 10.1080/10426914.2015.1019127.

[6] A.B. Chattopadhyay, A. Bose, and A.K. Chattopdhyay. Improvements in grinding steels by cryogenic cooling. *Precision Engineering*, 7(2):93–98, 1985. doi: 10.1016/0141-6359(85)90098-4.

[7] P.P. Reddy and A. Ghosh. Some critical issues in cryo-grinding by a vitrified bonded alumina wheel using liquid nitrogen jet. *Journal of Materials Processing Technology*, 229: 29–337, 2016. doi: 10.1016/j.jmatprotec.2015.09.040.

[8] M. Vijay Kumar, B.J. Kiran Kumar, and N. Rudresha. Optimization of machining parameters in CNC turning of stainless steel (EN19) by Taguchi's orthogonal array experiments. *Materials Today: Proceedings*, 5(5):11395–11407, 2018. doi: 10.1016/j.matpr.2018.02.107.

[9] M. Mia and N.R. Dhar. Optimization of surface roughness and cutting temperature in high-pressure coolant-assisted hard turning using Taguchi method. *The International Journal of Advanced Manufacturing Technology*, 88(1-4):739–753, 2017. doi: 10.1007/s00170-016-8810-2.

[10] G.M. Patel, Jagadish, R. Suresh Kumar, and N.V.S. Naidu. Optimization of abrasive water jet machining for green composites using multi-variant hybrid techniques. In K.Gupta, M.Kumar Gupta (eds.) *Optimization of Manufacturing Processes*, pages 129–162, Springer, 2020. doi: 10.1007/978-3-030-19638-7_6.

[11] D. Saravanakumar, B. Mohan, and T. Muthuramalingam. Application of response surface methodology on finding influencing parameters in servo pneumatic system. *Measurement*, 54:40–50, 2014. doi: 10.1016/j.measurement.2014.04.017.

[12] N.S. Jaddi and S. Abdullah. A cooperative-competitive master-slave global-best harmony search for ANN optimization and water-quality prediction. *Applied Soft Computing*, 51:209–224, 2017. doi: 10.1016/j.asoc.2016.12.011.

[13] A.S. Prasanth, R. Ramesh, and G. Palaniappan. Taguchi grey relational analysis for multi-response optimization of wear in co-continuous composite. *Materials*, 11(9):1743, 2018. doi: 10.3390/ma11091743.

[14] R. Manivannan and M.Pradeep Kumar. Multi-attribute decision-making of cryogenically cooled micro-EDM drilling process parameters using TOPSIS method. *Materials and Manufacturing Processes*, 32(2):209–215, 2017. doi: 10.1080/10426914.2016.1176182.

[15] J.S. Vesterstrøm and J. Riget. Particle swarms: Extensions for improved local, multi-modal, and dynamic search in numerical optimization. Master's Thesis, Dept. of Computer Science, University of Aarhus, Denmark, May, 2002.

[16] G. Meral, M. Sarıkaya, M. Mia, H. Dilipak, U. Şeker, and M.K. Gupta. Multi-objective optimization of surface roughness, thrust force, and torque produced by novel drill geometries using Taguchi-based GRA. *The International Journal of Advanced Manufacturing Technology*, 101(5-8):1595–1610, 2019. doi: 10.1007/s00170-018-3061-z.

[17] M. Priyadarshini, I. Nayak, J. Rana and P.P. Tripathy. Multi-objective optimization of turning process using fuzzy-TOPSIS analysis. *Materials Today: Proceedings*, March, 2020. doi: 10.1016/j.matpr.2020.02.847.

[18] M. Alhabo and L. Zhang. Multi-criteria handover using modified weighted TOPSIS methods for heterogeneous networks. *IEEE Access*, 6:40547–40558, 2018. doi: 10.1109/ACCESS.2018.2846045.

[19] P.B. Zaman, S. Saha, and N.R. Dhar. Hybrid Taguchi-GRA-PCA approach for multi-response optimisation of turning process parameters under HPC condition. *International Journal of Machining and Machinability of Materials*, 22(3-4):281–308, 2020. doi: 10.1504/IJMMM.2020.107059.

[20] N. Li, Y.J. Chen, and D.D. Kong. Multi-response optimization of Ti-6Al-4V turning operations using Taguchi-based grey relational analysis coupled with kernel principal component analysis. *Advances in Manufacturing*, 7(2):142–154, 2019. doi: 10.1007/s40436-019-00251-8.

[21] P. Umamaheswarrao, D.R. Raju, K.N.S. Suman, and B.R. Sankar. Multi objective optimization of process parameters for hard turning of AISI 52100 steel using Hybrid GRA-PCA. *Procedia Computer Science*, 133:703–710, 2018. doi: 10.1016/j.procs.2018.07.129.

[22] P.B. Patole and V.V. Kulkarni. Experimental investigation and optimization of cutting parameters with multi response characteristics in MQL turning of AISI 4340 using nano fluid. *Cogent Engineering*, 4(1):1303956, 2017. doi: 10.1080/23311916.2017.1303956.

[23] R. Viswanathan, S. Ramesh, S. Maniraj, and V. Subburam. Measurement and multi-response optimization of turning parameters for magnesium alloy using hybrid combination of Taguchi-GRA-PCA technique. *Measurement*, 159:107800, 2020. doi: 10.1016/j.measurement.2020.107800.

[24] S. Ramesh, R. Viswanathan and S. Ambika. Measurement and optimization of surface roughness and tool wear via grey relational analysis, TOPSIS and RSA techniques. *Measurement*, 78:63–72, 2016. doi: 10.1016/j.measurement.2015.09.036.

[25] A. Palanisamy and T. Selvaraj. Optimization of turning parameters for surface integrity properties on Incoloy 800H superalloy using cryogenically treated multi-layer CVD coated tool. *Surface Review and Letters*, 26(02):1850139, 2019. doi: 10.1142/S0218625X18501391.

[26] R. Thirumalai and J.S. Senthilkumaar. Multi-criteria decision making in the selection of machining parameters for Inconel 718. *Journal of Mechanical Science and Technology*, 27(4):1109–1116, 2013. doi: 10.1007/s12206-013-0215-7.

[27] M. Mia. Mathematical modeling and optimization of MQL assisted end milling characteristics based on RSM and Taguchi method. *Measurement*, 121:249–260, 2018. doi: 10.1016/j.measurement.2018.02.017.

[28] P.J. Ross. *Taguchi Techniques for Quality Engineering*. McGraw-Hill, New York, 2 edition, 1996.

[29] A. Palanisamy and T. Selvaraj. Optimization of machining parameters for dry turning of Incoloy 800H using Taguchi-based grey relational analysis. *Materials Today: Proceedings*, 5(2):7708–7715, 2018. doi: 10.1016/j.matpr.2017.11.447.

[30] K. Pearson. On lines and planes of closest fit to systems of points in space. *The London, Edinburgh, and Dublin Philosophical Magazine and Journal of Science*, 2(11):559–572, 1901. doi: 10.1080/14786440109462720.

[31] H. Hotelling. Analysis of a complex of statistical variables into principal components. *Journal of Educational Psychology*, 24(6):417–441, 1993. doi: 10.1037/h0071325.

[32] M. Mia, M.K. Gupta, J.A. Lozano, D. Carou, D.Y. Pimenov, G. Królczyk, A.M. Khan, and N.R. Dhar. Multi-objective optimization and life cycle assessment of eco-friendly cryogenic N_2 assisted turning of Ti-6Al-4V. *Journal of Cleaner Production*, 210: 121-133, 2019. doi: 10.1016/j.jclepro.2018.10.334.

[33] M.A. Khan, S.H.I. Jaffery, M. Khan, M. Younas, S.I. Butt, R. Ahmad, and S.S. Warsi. Multi-objective optimization of turning titanium-based alloy Ti-6Al-4V under dry, wet, and cryogenic conditions using gray relational analysis (GRA). *The International Journal of Advanced Manufacturing Technology*, 106(9-10):3897–3911, 2020. doi: 10.1007/s00170-019-04913-6.

[34] M.J. Bermingham, J. Kirsch, S. Sun, S. Palanisamy, and M.S. Dargusch. New observations on tool life, cutting forces and chip morphology in cryogenic machining Ti-6Al-4V. *International Journal of Machine Tools and Manufacture*, 51(6):500–511, 2011. doi: 10.1016/j.ijmachtools.2011.02.009.

[35] M. Strano, E. Chiappini, S. Tirelli, P. Albertelli, and M. Monno. Comparison of Ti6Al4V machining forces and tool life for cryogenic versus conventional cooling. *Proceedings of the Institution of Mechanical Engineers, Part B: Journal of Engineering Manufacture*, 227(9):1403–1408, 2013. doi: 10.1177/0954405413486635.

[36] H.S. Lu, C.K. Chang, N.C. Hwang, and C.T. Chung. Grey relational analysis coupled with principal component analysis for optimization design of the cutting parameters in high-speed end milling. *Journal of Materials Processing Technology*, 209(8):3808–3817, 2009. doi: 10.1016/j.jmatprotec.2008.08.030.

[37] L.S. Ahmed and M.Pradeep Kumar. Multiresponse optimization of cryogenic drilling on Ti-6Al-4V alloy using TOPSIS method. *Journal of Mechanical Science and Technology*, 30(4):1835–1841, 2016. doi: 10.1007/s12206-016-0340-1.